On the Relation of the Coronal X-ray Source and the Footpoints

Marina Battaglia
Arnold Benz

ETH
Eidgenössische Technische Hochschule Zürich
Swiss Federal Institute of Technology, Zürich

What relation between coronal source and footpoint sources?

Toy Model

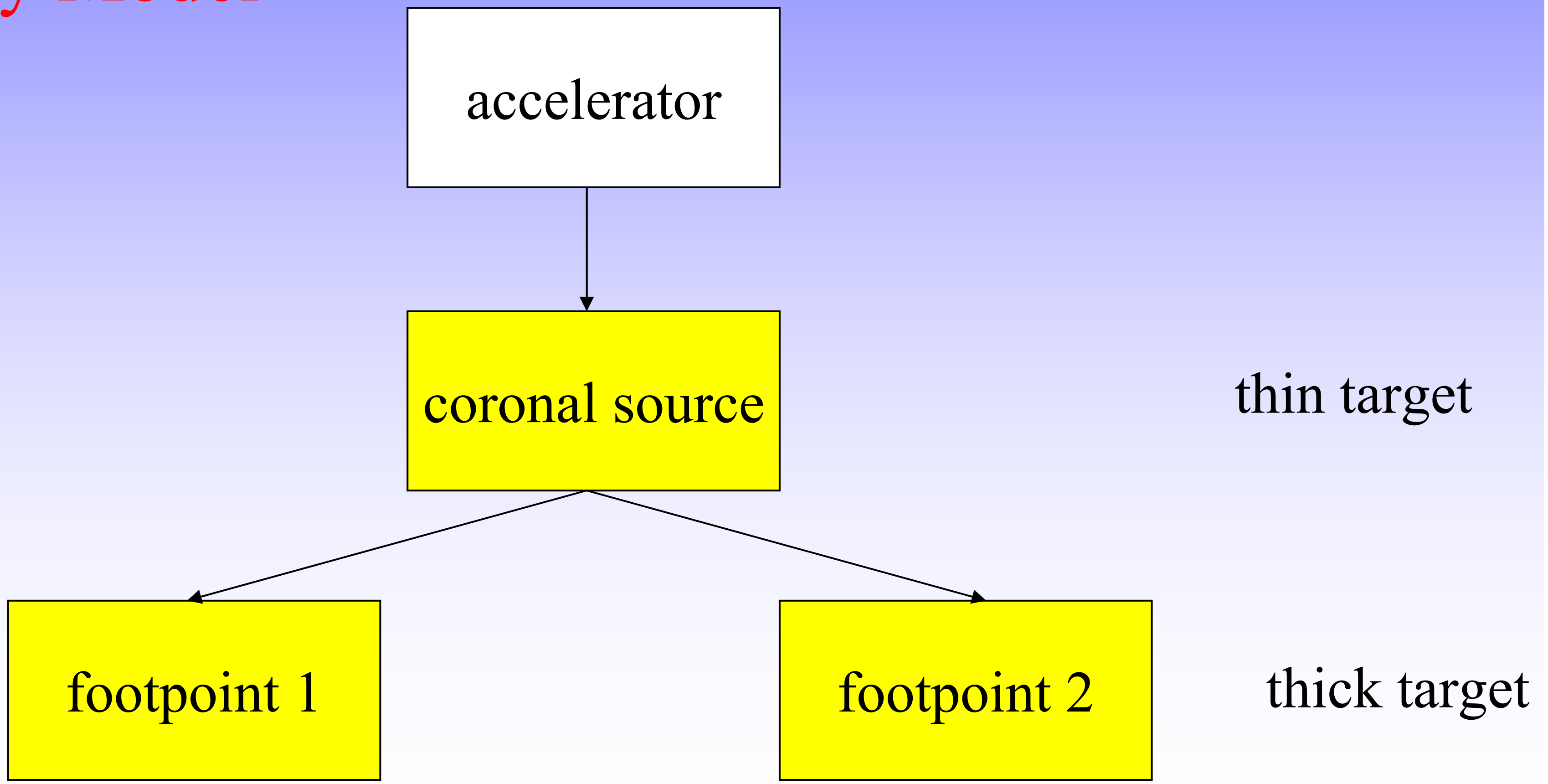

Predictions of Toy Model

Relation between coronal source and footpoints

- simultaneous evolution
- soft-hard-soft behavior in coronal source
- difference in spectral index = 2
- same spectral index in two footpoints

Expect tight relation !

If not

- transport effect: Coulomb collisions, electric field
- particle containment in coronal source:
  anomalous collisions, electric field

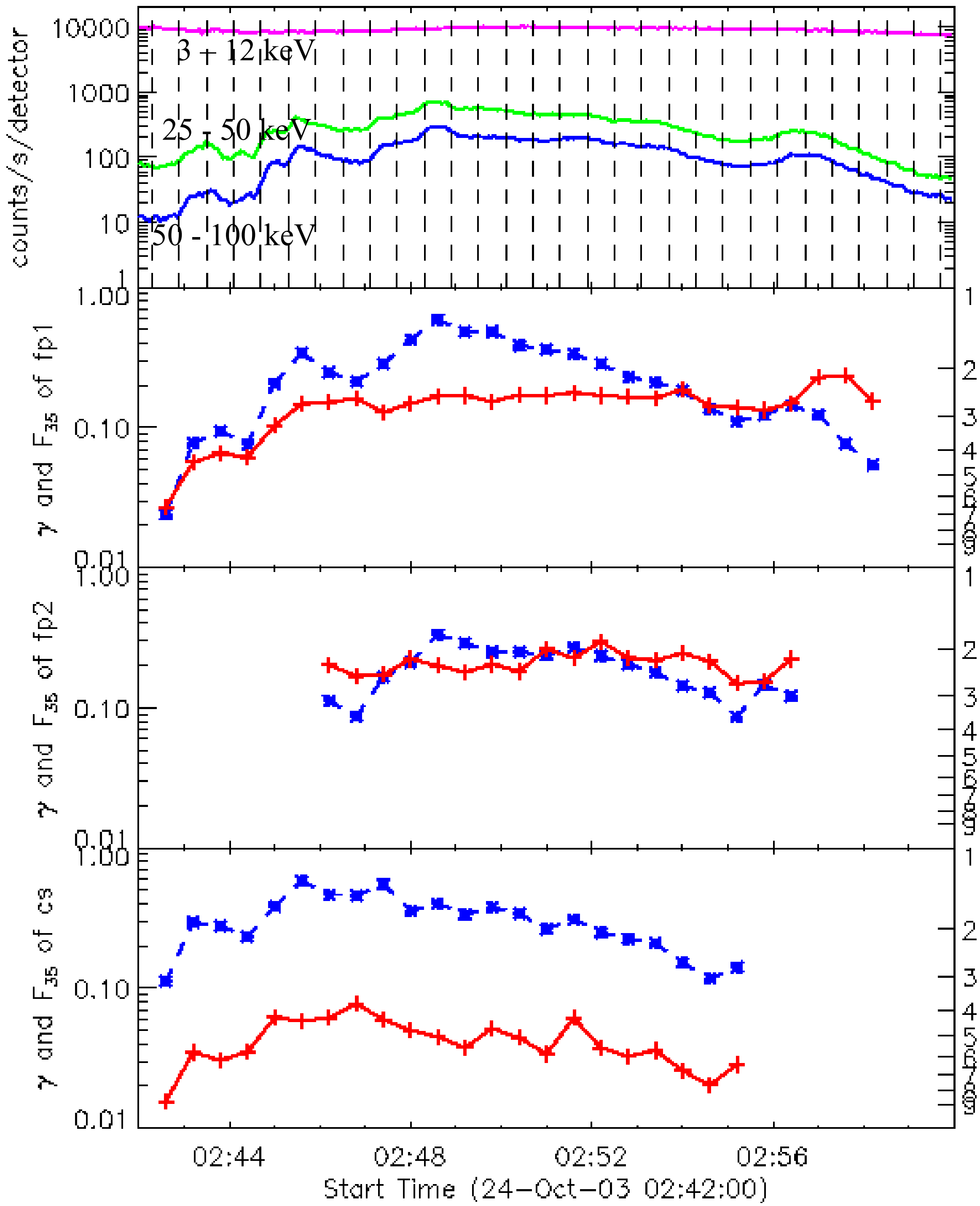

Full Sun

Footpoint 1

Footpoint 2

Coronal Source

— F_{35}

— γ

Battaglia & B. 2006

Results

Coronal source

- dominant thermal component
- weak and soft non-thermal component
- soft-hard-soft behavior
- evolves nearly simultaneously to footpoints

Results

Footpoint sources

- γ between 0 and 4 harder than in coronal source

- same spectral index in footpoints in 4 of 5 flares

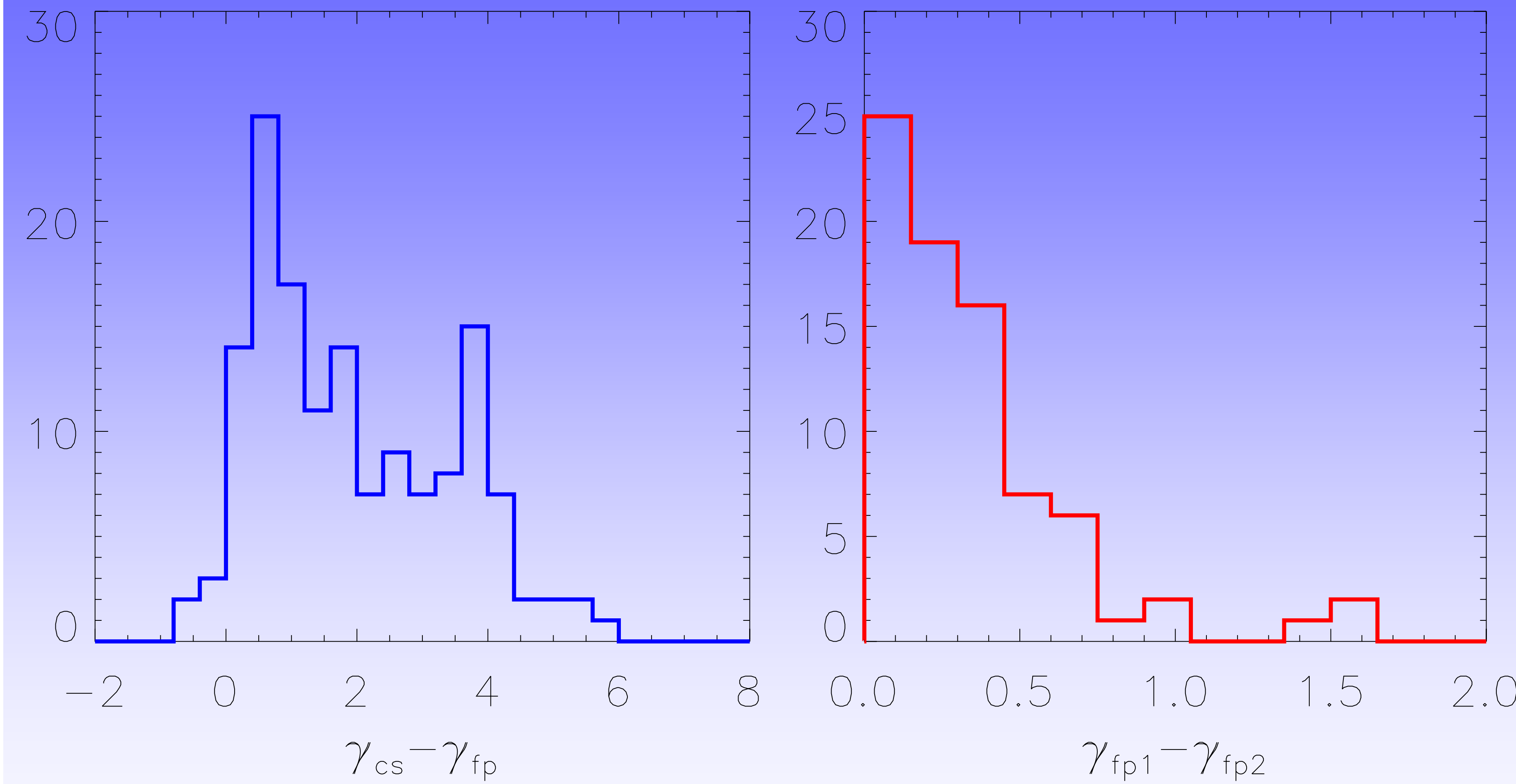

Footpoint sources:

- between 0 and 4 harder than in coronal source
- same spectral index in 4 footpoint pairs of 5 flares

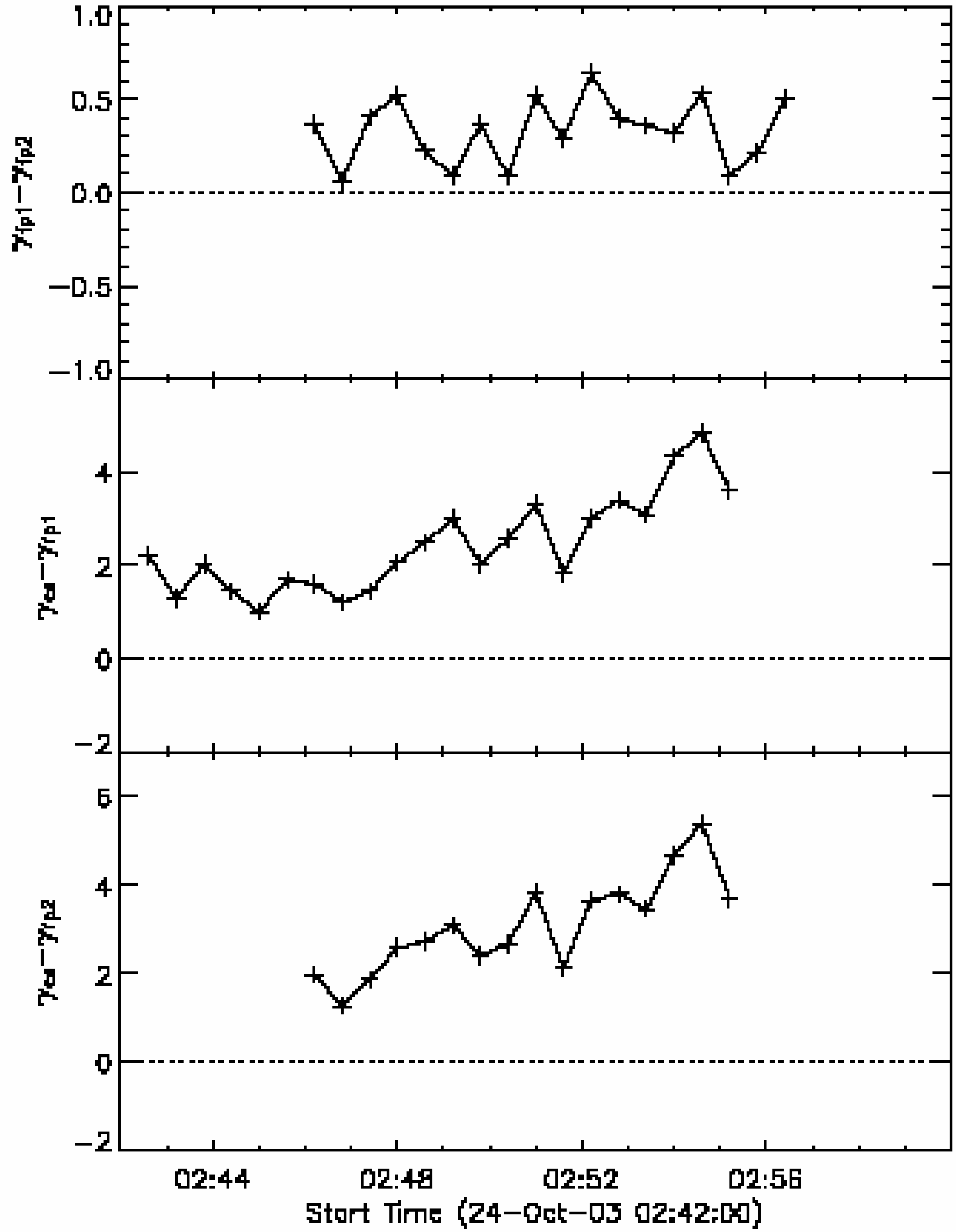

One case out of 5 !

Footpoint 1 – 2

Footpoint 1 is softer, larger in flux and area

Coronal source – Footpoint 1

Coronal source – Footpoint 1

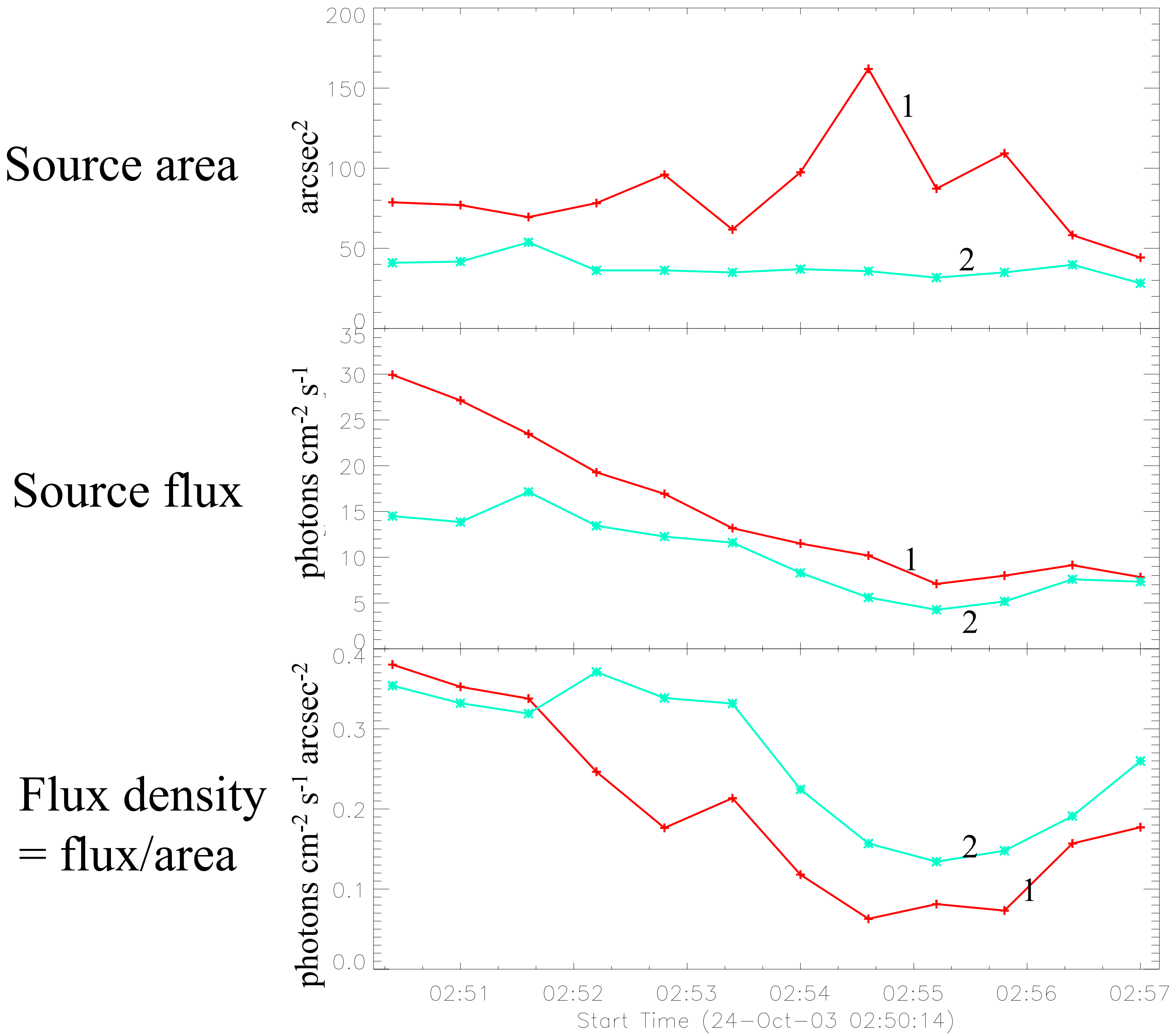

Source area
Source flux
Flux density
= flux/area
arcsec^2
photons cm^{-2} s^{-1}
photons cm^{-2} s^{-1} arcsec^{-2}
1
2
Start Time (24-Oct-03 02:50:14)
02:51
02:52
02:53
02:54
02:55
02:56
02:57

Flux density = flux / area

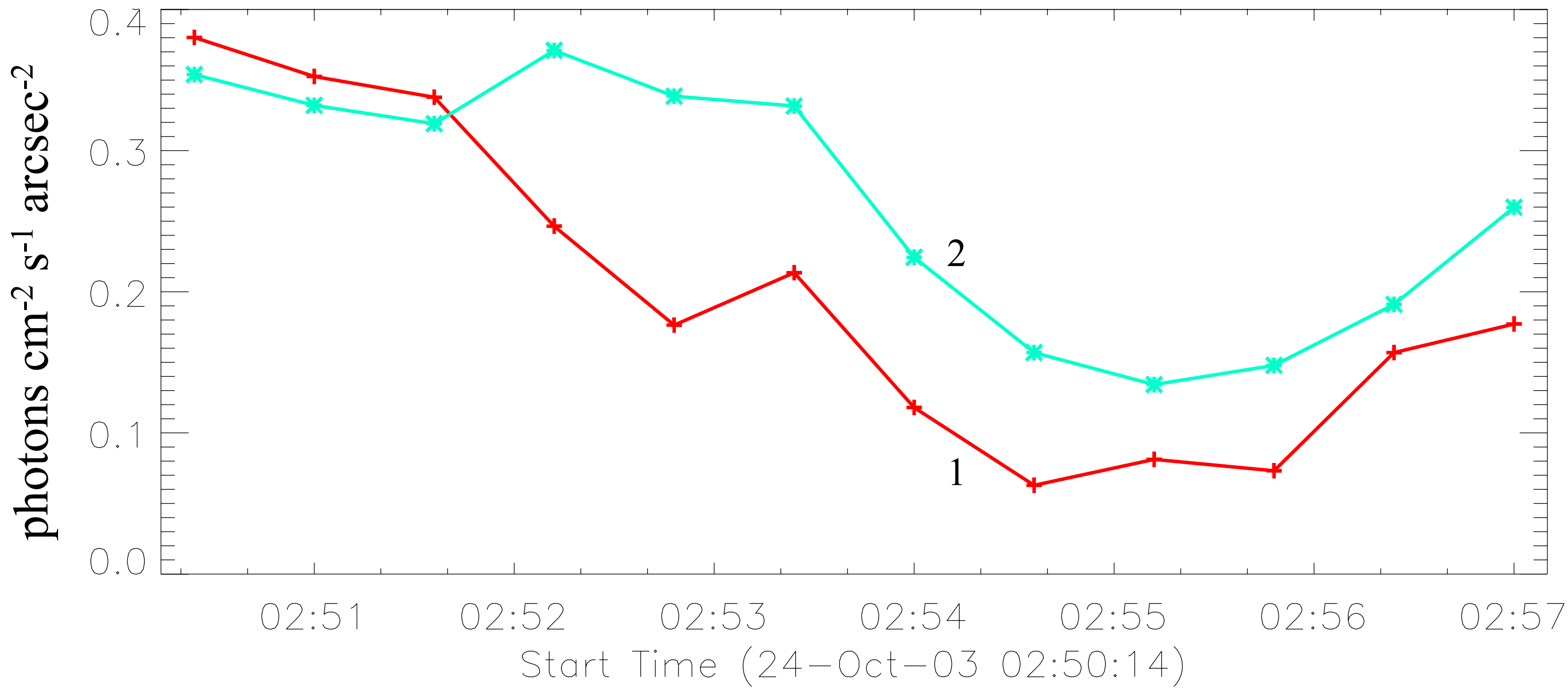

1. **Same flux density within factor of 2 at peak**
2. **Softer footpoint (1) has smaller flux density later in flare**

1. Footpoints have similar flux densities

(in one case)

Electron flux at one footpoint:

$$F_{fp} = \iiint f(v,x,y)dv\,dx\,dy = A\,\bar{n}_{prec} \langle v_e \rangle \qquad [\text{electrons s}^{-1}]$$

Current produced by electrons (neglect ions):

$$j_e = -e\,\bar{n}_{prec} \langle v_e \rangle \quad = -e\,F_{fp} / A$$

1. Footpoints have similar flux densities

(in one case)

Electron flux at one footpoint:

$$F_{fp} = \iiint f(v,x,y)dv\,dx\,dy = A\,\bar{n}_{prec} \langle v_e \rangle \qquad [\text{electrons s}^{-1}]$$

Current produced by electrons (neglect ions):

$$j_e = -e\,\bar{n}_{prec} \langle v_e \rangle = -e\,F_{fp} / A$$

$$= -j_{ret} = e\,n_{th}\,\Delta v < e\,n_{th}\,c_{is}$$

where $\Delta v = \langle v_i \rangle - \langle v_e \rangle$ and $c_{is} = \sqrt{kT_e/m_i}$.

Using $\Delta v \approx \langle v \rangle$, the flux density is limited by

$$F_{fp}/A < n_{th}\,c_{is} \qquad [\text{electrons s}^{-1}\text{ cm}^{-2}]$$

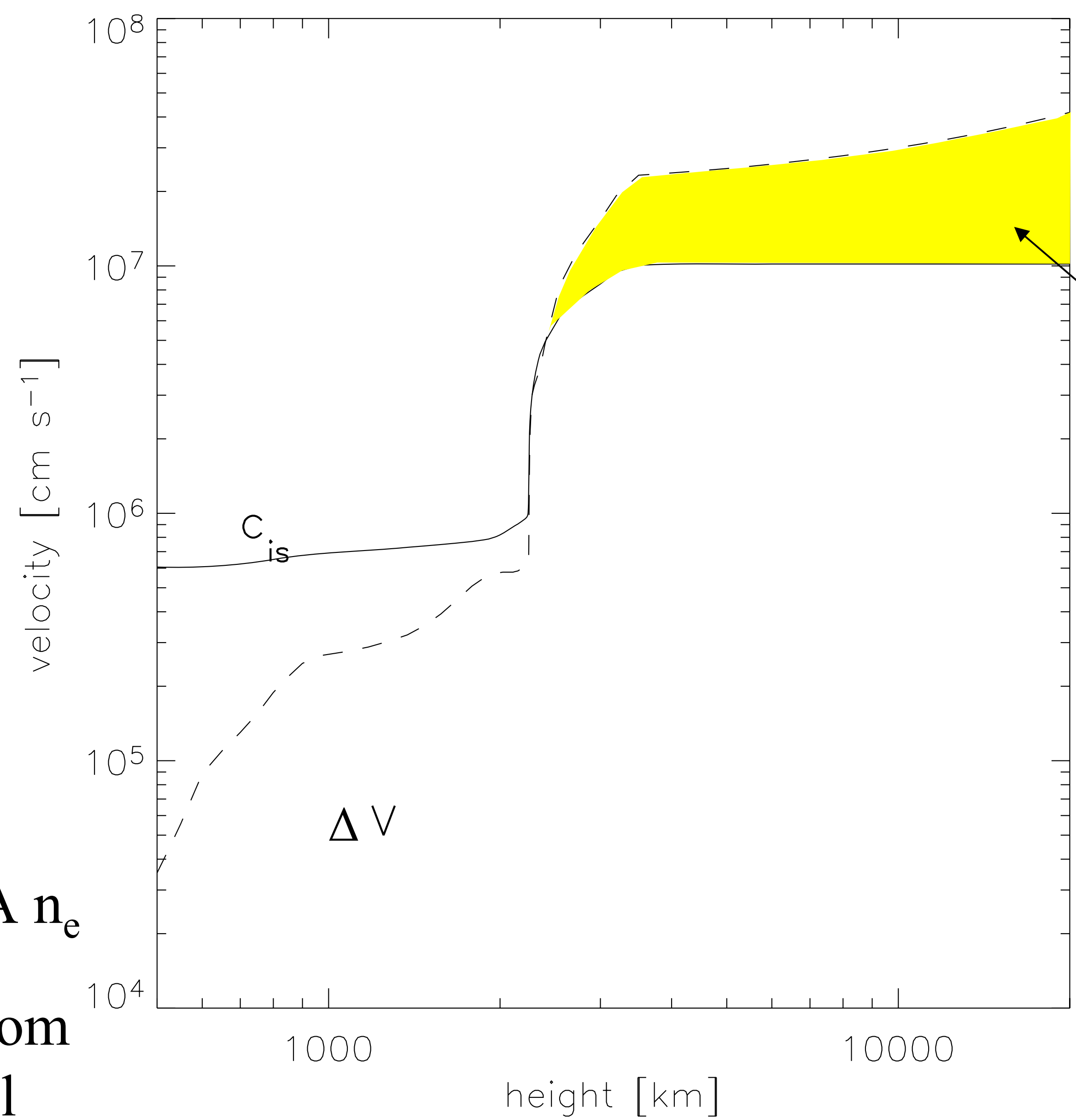

Unstable return current

↓

large resistance

↓

large electric field

↓

similar flux density

$\Delta V = F_{fp} / A\, n_e$

n_e and T from FAL model

2. Larger footpoint has more flux, lower flux density and is softer

Interpretation:

- Lower flux density means smaller j_e
- Smaller j_e suggests smaller return current and smaller electric field (Ohm's law).
- Less less electric field, less hardening, softer source.

2. Larger footpoint has more flux, lower flux density and is softer

BUT alternative interpretation:

- Lower flux density suggests smaller evaporation.
- Less evaporation means less dense loop, fewer Coulomb collisions in transport.
- Less collisions, less spectral hardening.
- Less hardening, softer source.

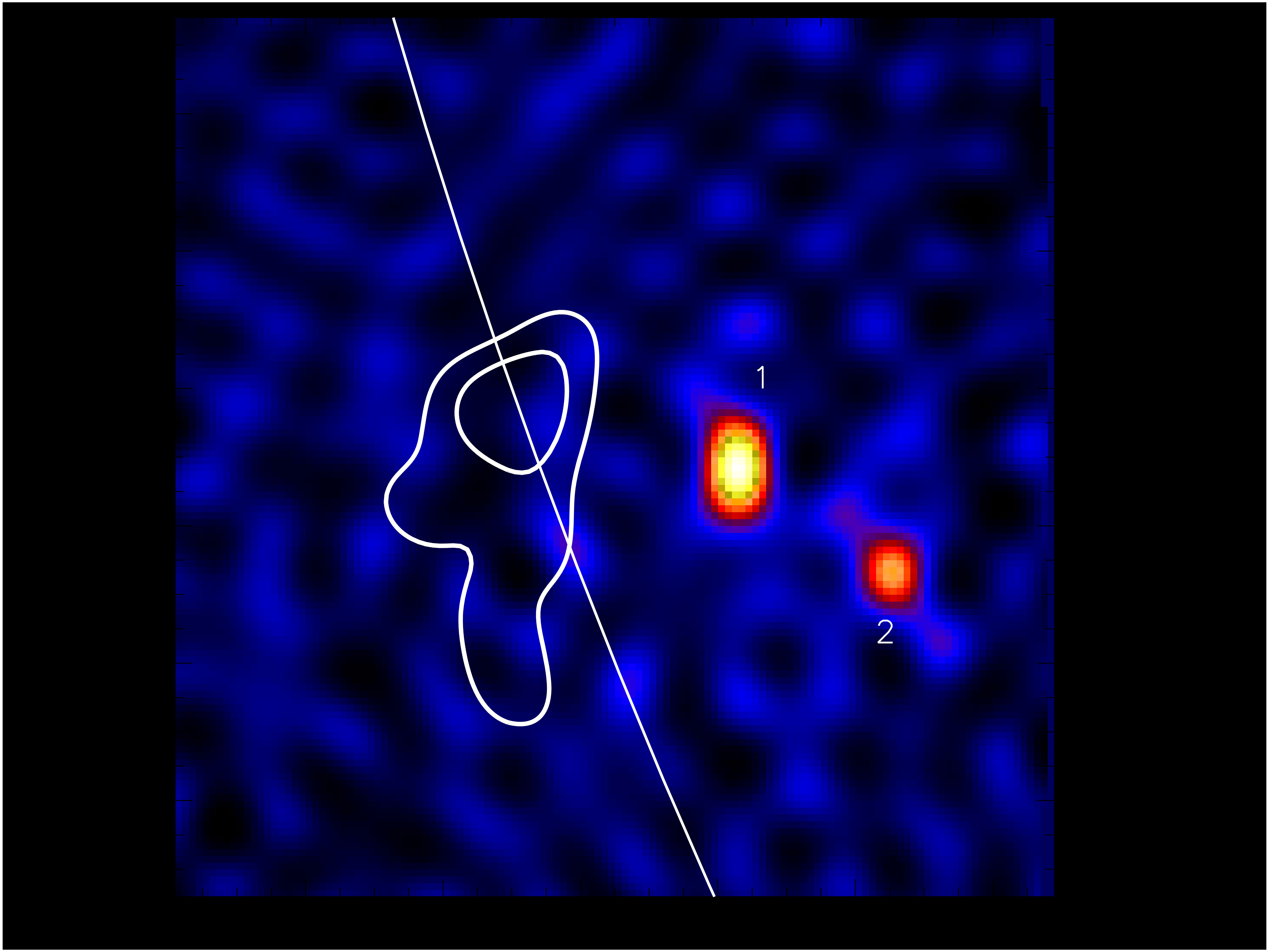
1
2

Transition from corona to footpoint?

- Can we distinguish the coronal source (accelerator?), propagation in loop, and thick target footpoint?
- Where is the transition from the soft coronal source to the hard footpoints?

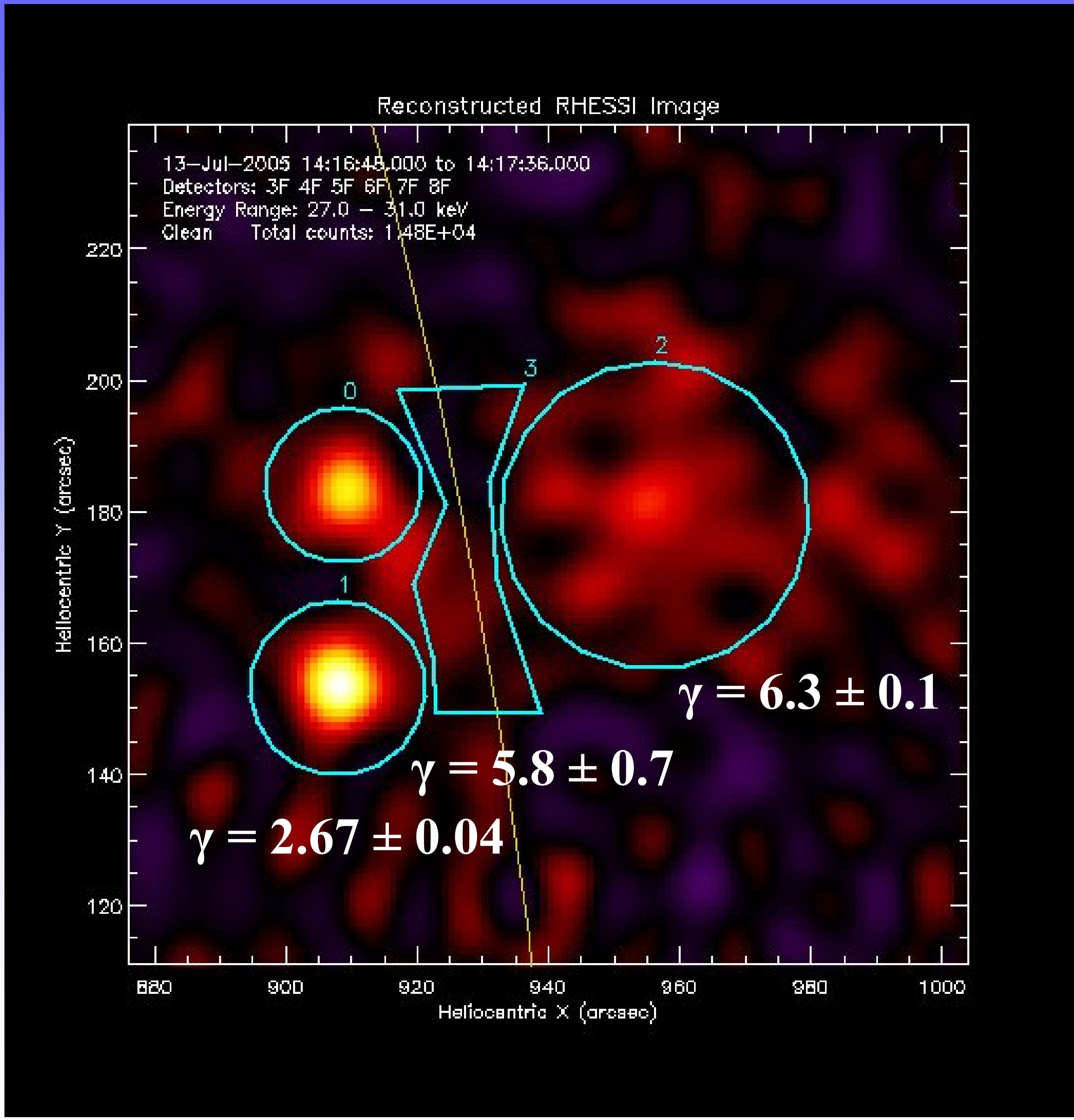

Transition region (3) has nearly coronal spectral index

↓

Transition is close to chromosphere

Results

Coronal source

soft-hard-soft behavior

simultaneous to footpoints

Footpoint sources

between 0 and 4 smaller than in coronal source

same spectral index in 4 of 5 flares

one exception is consistent with collisional transport effect

Transition from coronal source to footpoints

near footpoints (consistent with electric field effect)

Comparison with Predictions

Relation between coronal source and footpoints

- simultaneous evolution **Yes**
- soft-hard-soft behavior **Yes** (not transport effect)
- difference in spectral index = 2 **NO** (transport effect)
- same spectral index in two footpoints **NO** (transport effect)

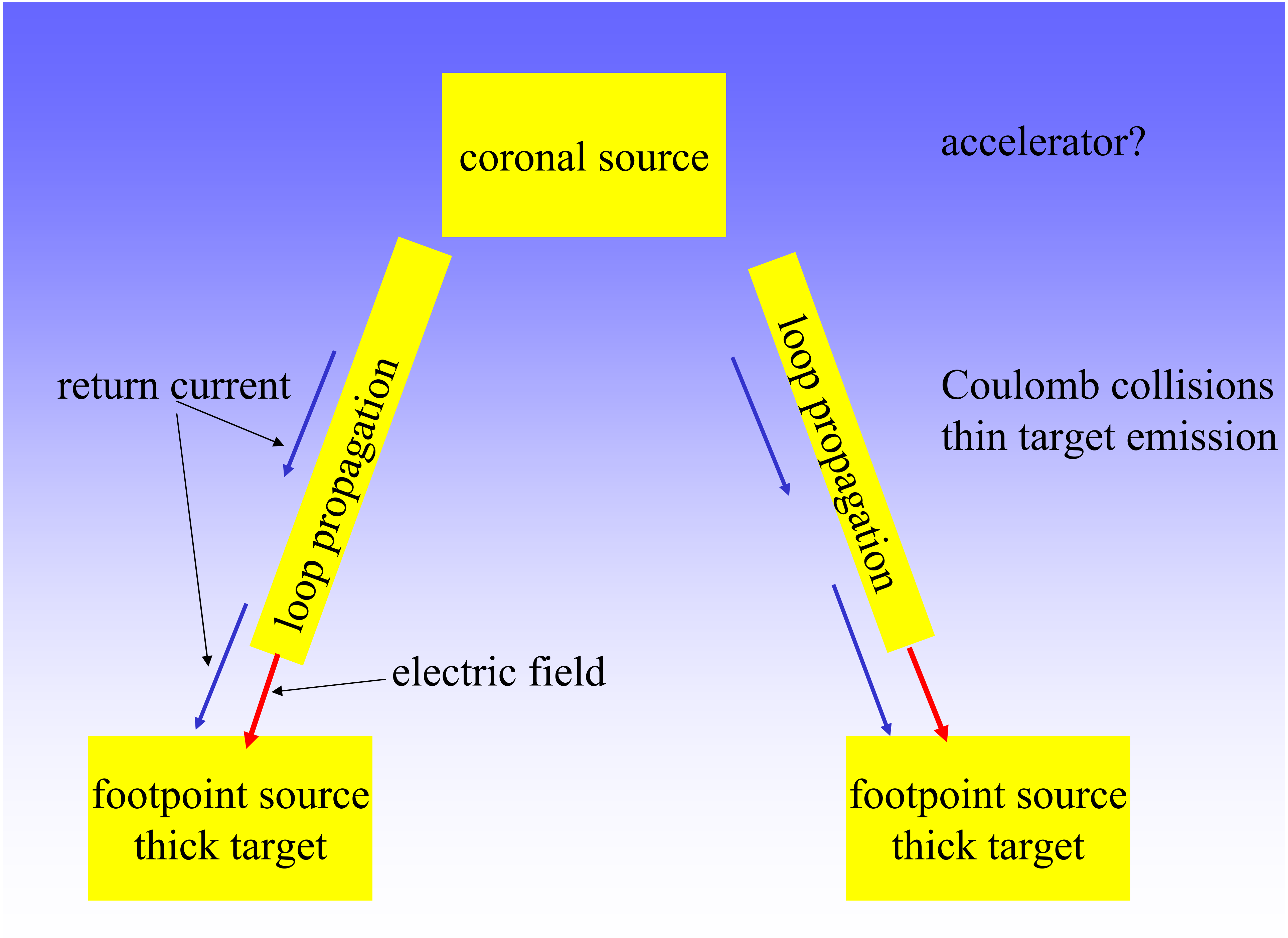
coronal source
accelerator?
return current
loop propagation
loop propagation
Coulomb collisions
thin target emission
electric field
footpoint source
thick target
footpoint source
thick target

Observations consistent with

- Accelerator in coronal source (shs)
- Transport effects (both collisions and electric field)
- Limitation of return current
- If return current, then electric field ∥B changing transport properties
- Electric field strongest in very low corona
- Transition to thick target very low in corona
- But also Coulomb collisions in loop

Method

Selection of 5 events with

- 3 sources
- near limb (R > 700“)
- larger than M1
- no pile up and no terrestrial electrons

Coronal source

- one source is softer and larger R

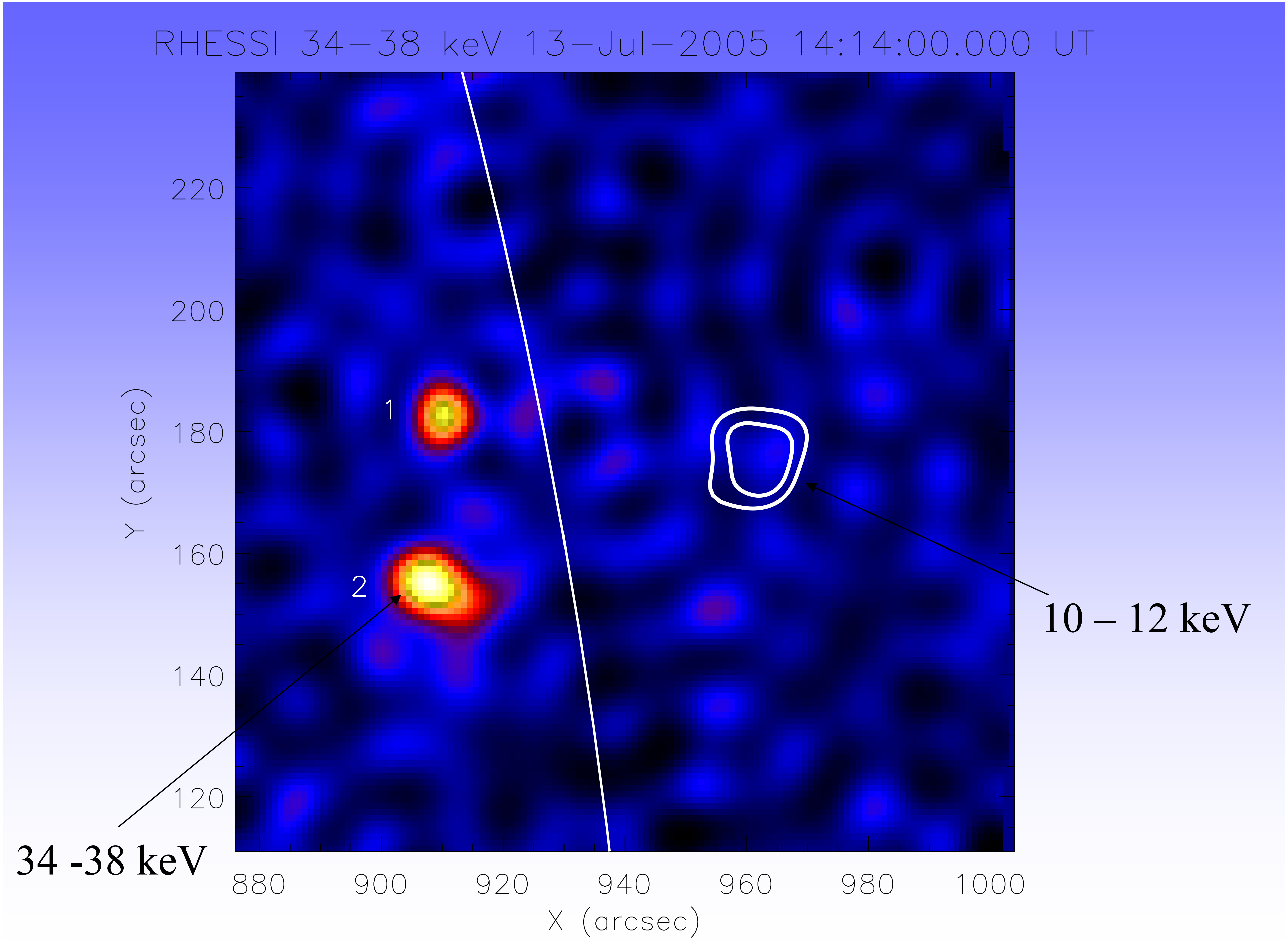
RHESSI 34−38 keV 13−Jul−2005 14:14:00.000 UT
Y (arcsec)
X (arcsec)
220
200
180
160
140
120
880
900
920
940
960
980
1000
1
2
10 – 12 keV
34 -38 keV

What relation between sources?

- Use imaging spectroscopy
- Define regions of interest

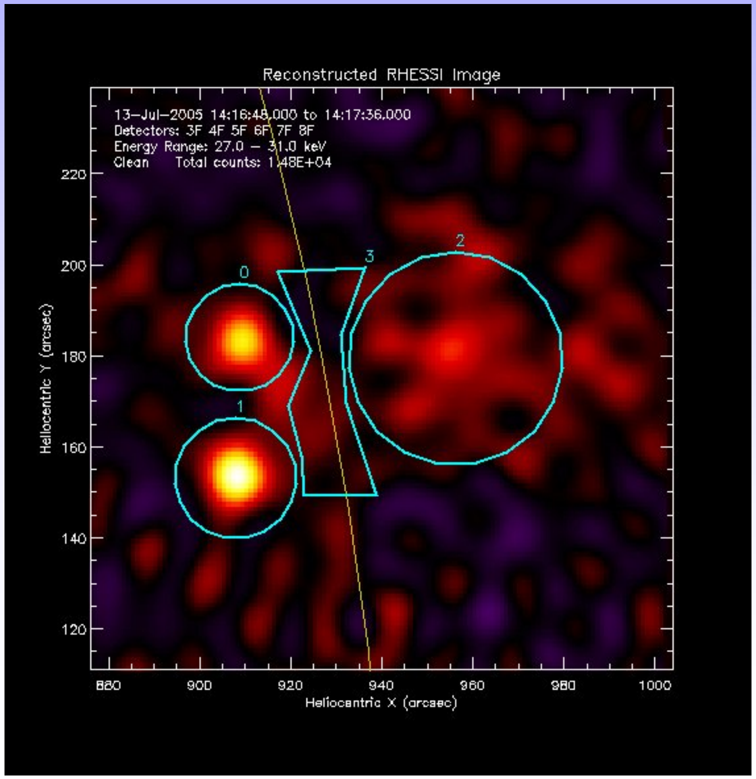

What relation between sources?

- Use imaging spectroscopy
- Define regions of interest
- Spectral fitting of regions in time

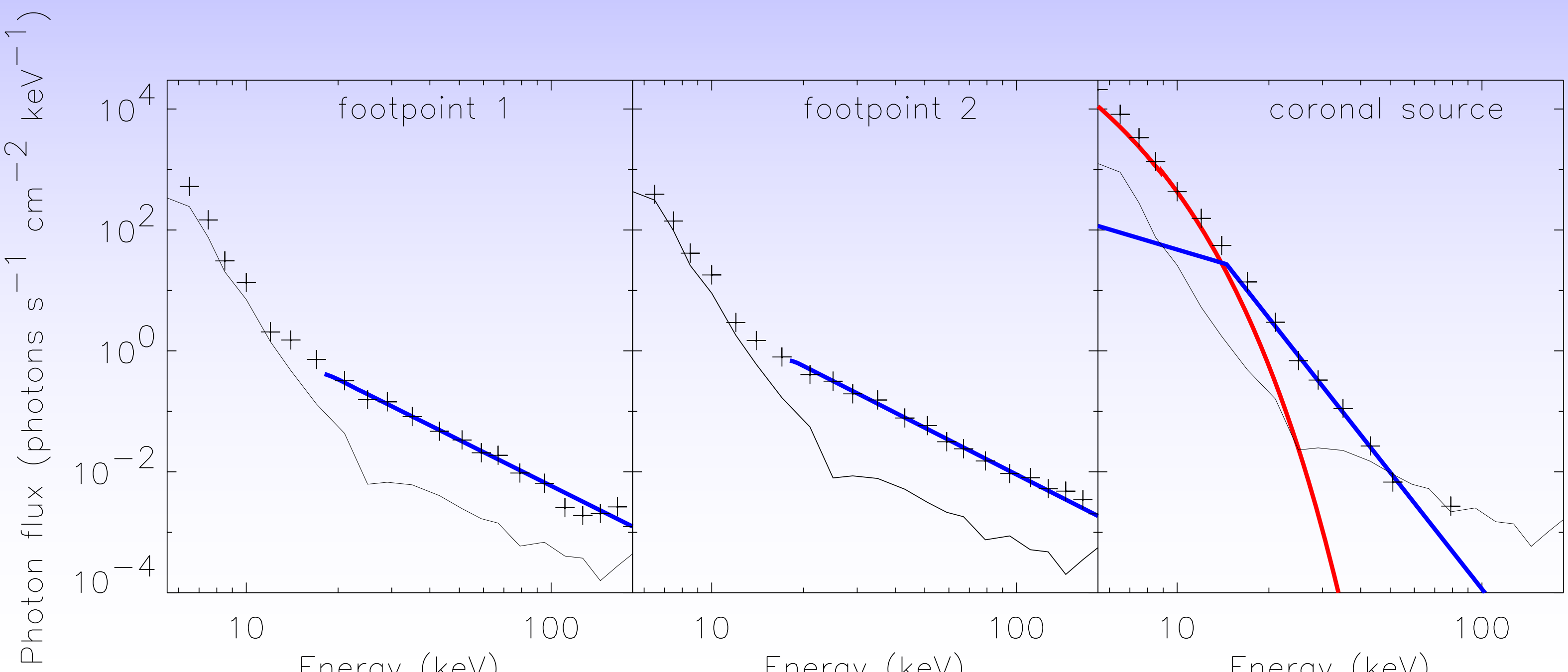

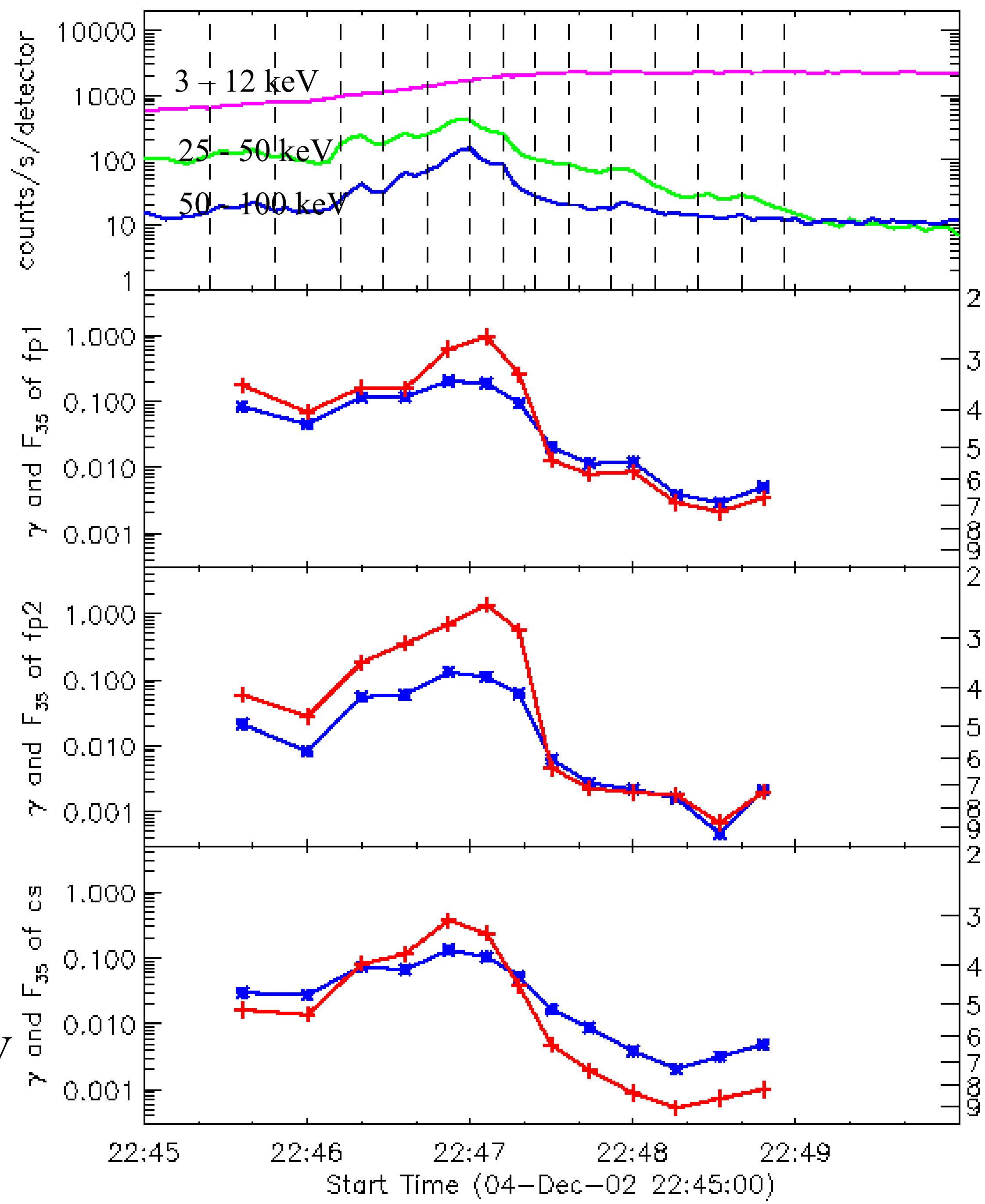

Full Sun

Footpoint 1

Footpoint 2

Coronal Source

$F_{35\ keV}$

γ

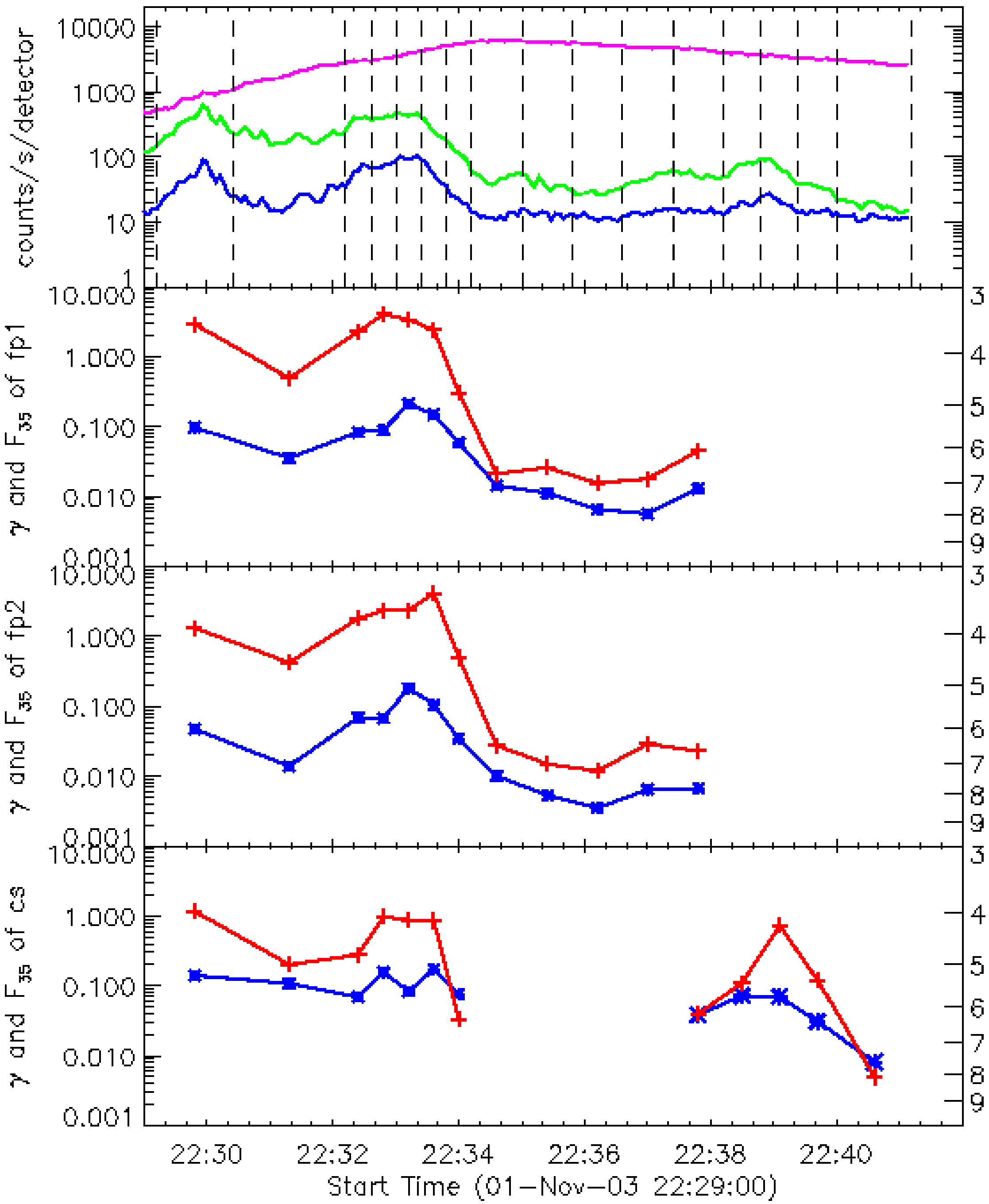

Full Sun

Footpoint 1

Footpoint 2

Coronal Source

— F_{35}

— γ

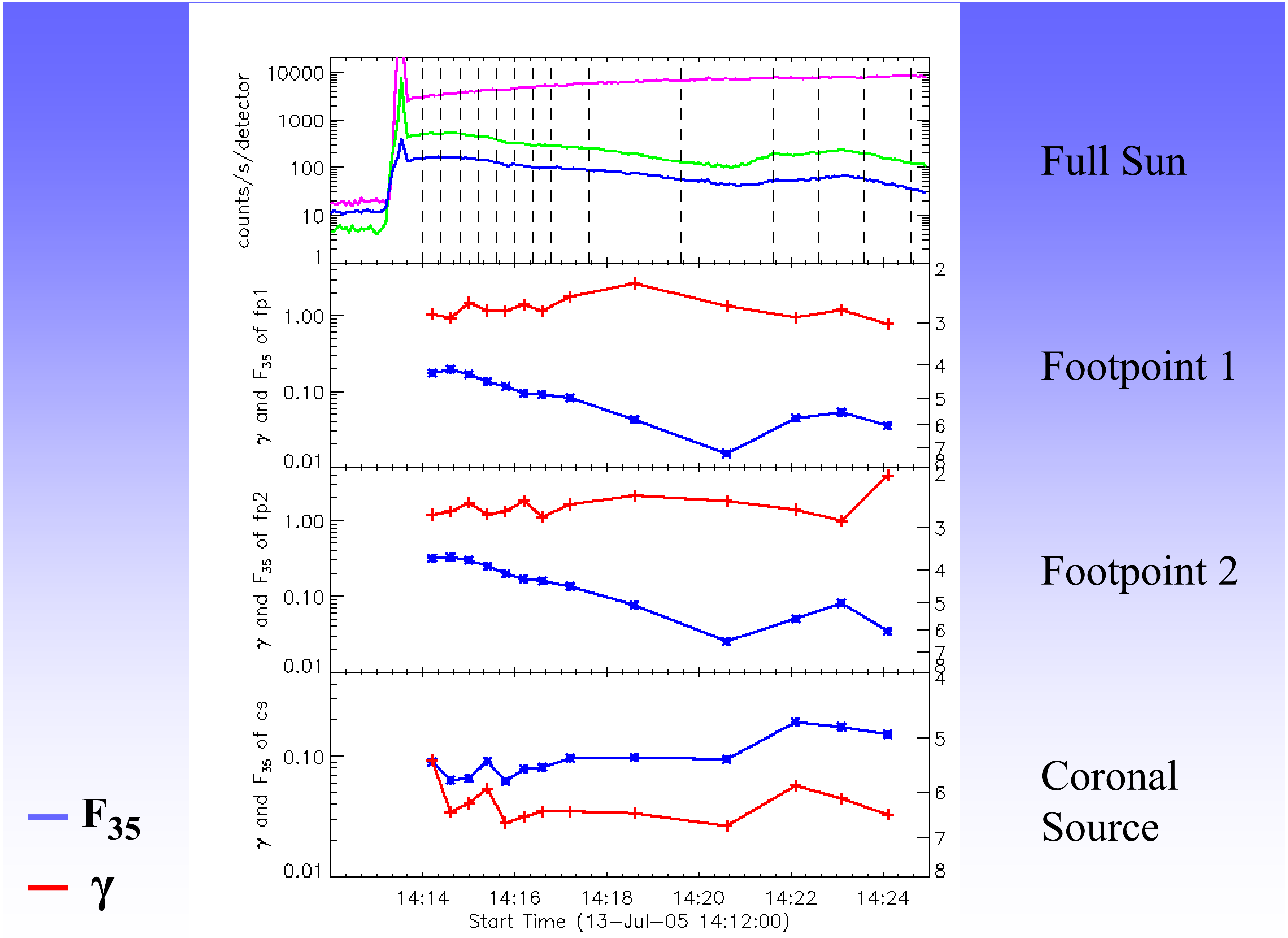

counts/s/detector
10000
1000
100
10
1
γ and F35 of fp1
1.00
0.10
0.01
γ and F35 of fp2
γ and F35 of cs
14:14
14:16
14:18
14:20
14:22
14:24
Start Time (13-Jul-05 14:12:00)
Full Sun
Footpoint 1
Footpoint 2
Coronal Source
F35
γ

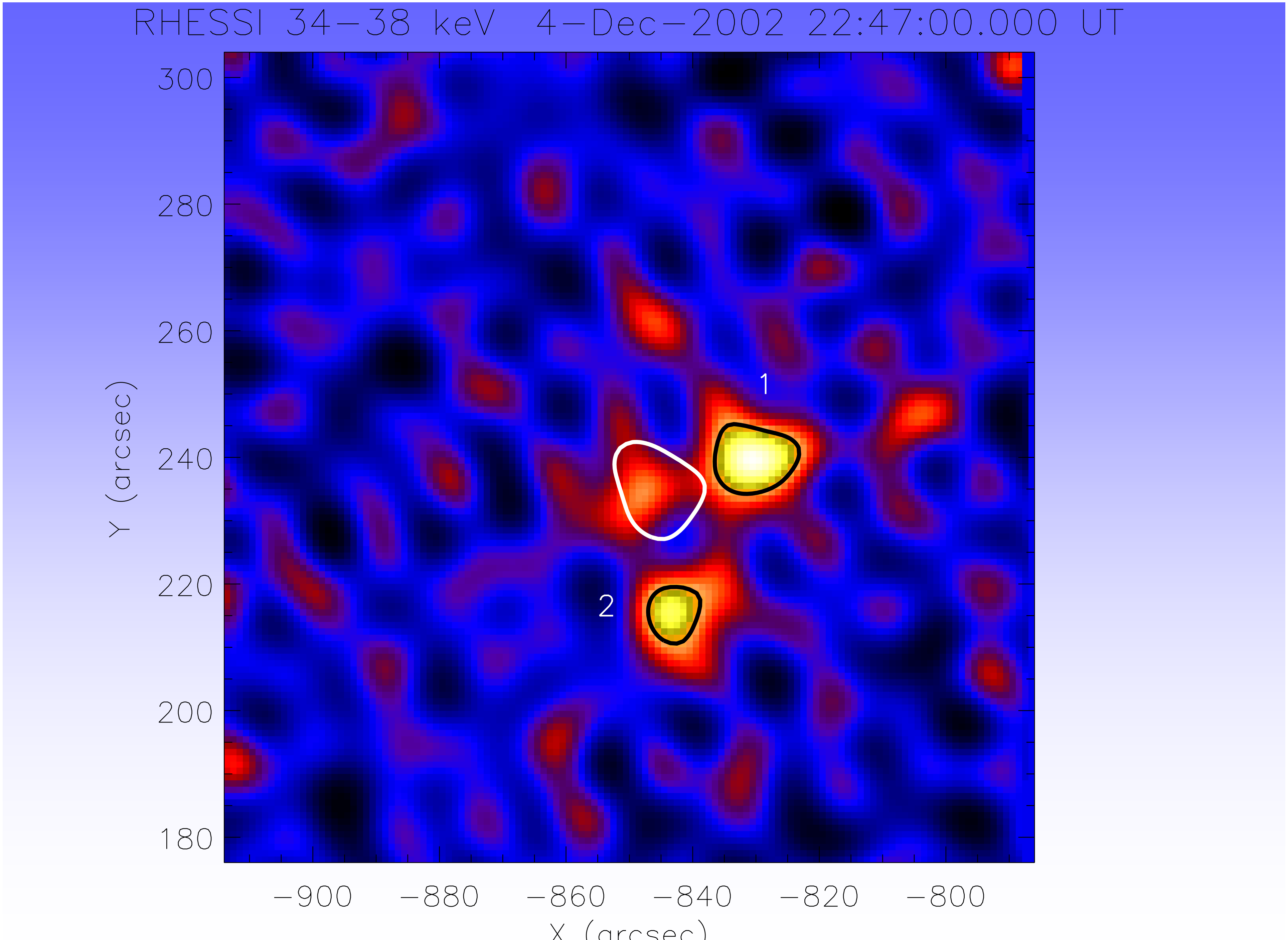
RHESSI 34−38 keV 4−Dec−2002 22:47:00.000 UT
300
280
260
240
220
200
180
Y (arcsec)
−900
−880
−860
−840
−820
−800
X (arcsec)
1
2

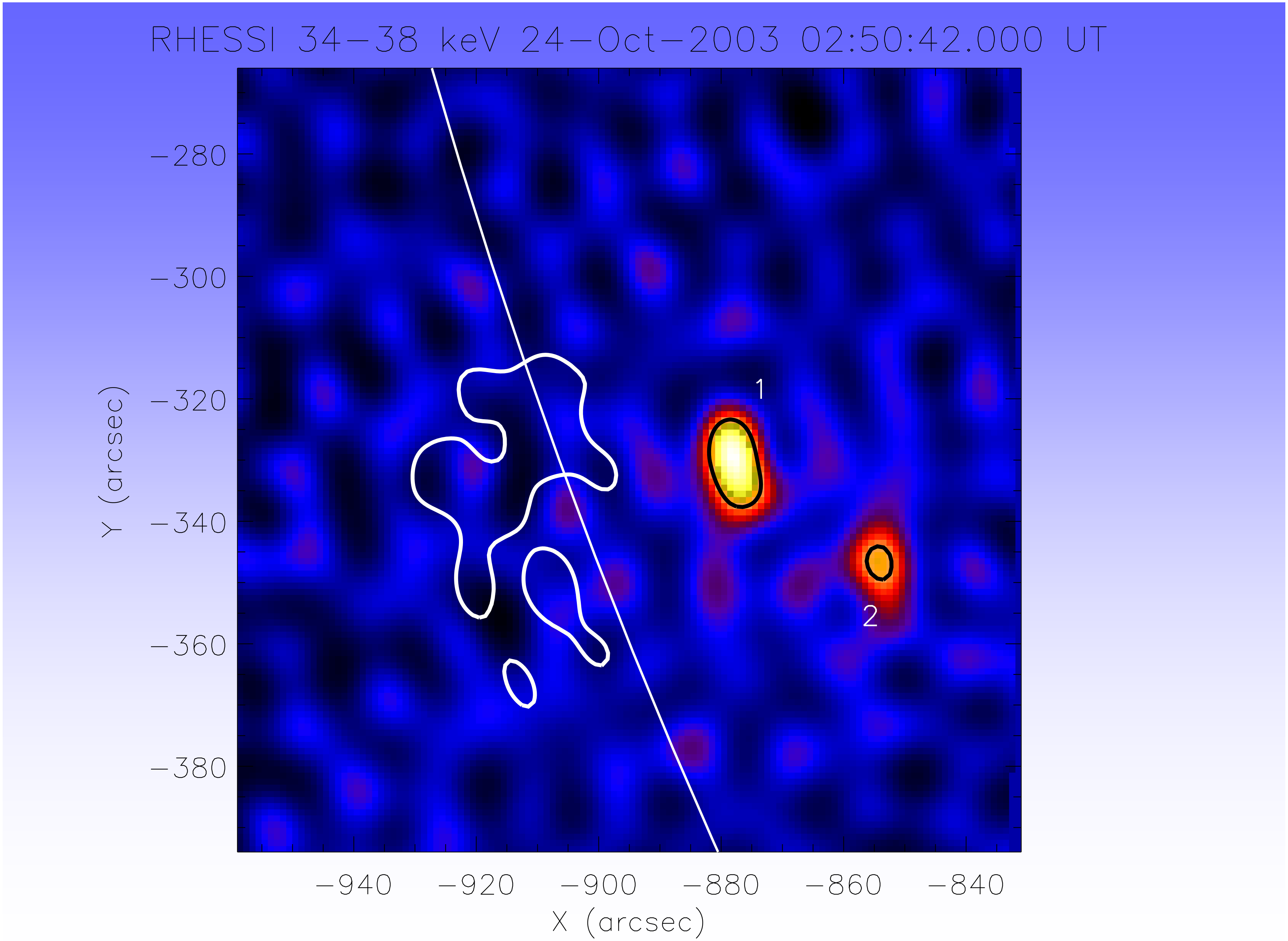
RHESSI 34-38 keV 24-Oct-2003 02:50:42.000 UT
Y (arcsec)
-280
-300
-320
-340
-360
-380
1
2
-940
-920
-900
-880
-860
-840
X (arcsec)

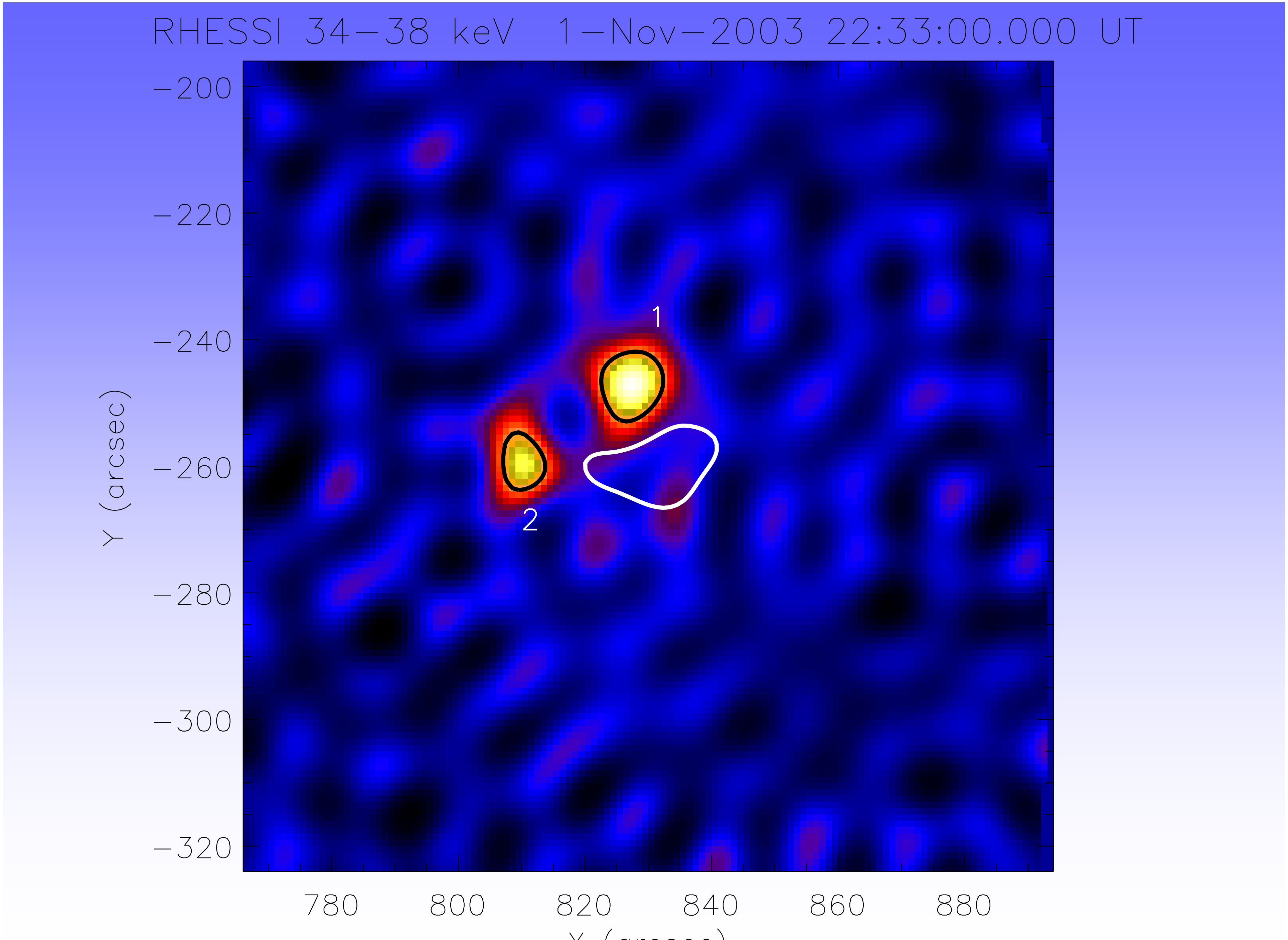
RHESSI 34–38 keV 1–Nov–2003 22:33:00.000 UT
Y (arcsec)
X (arcsec)
−200
−220
−240
−260
−280
−300
−320
780
800
820
840
860
880
1
2

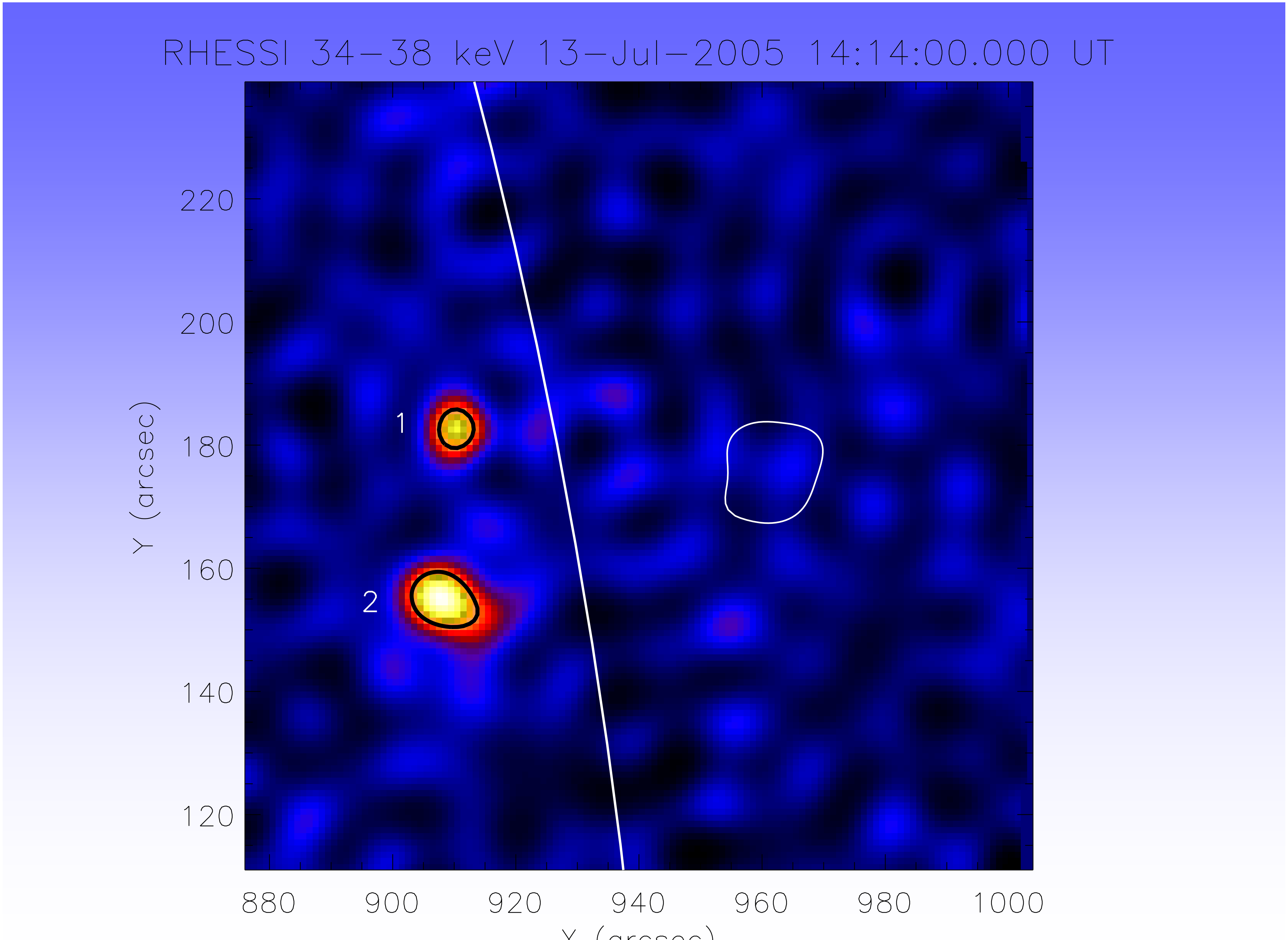
RHESSI 34-38 keV 13-Jul-2005 14:14:00.000 UT
220
200
180
160
140
120
Y (arcsec)
1
2
880
900
920
940
960
980
1000
X (arcsec)

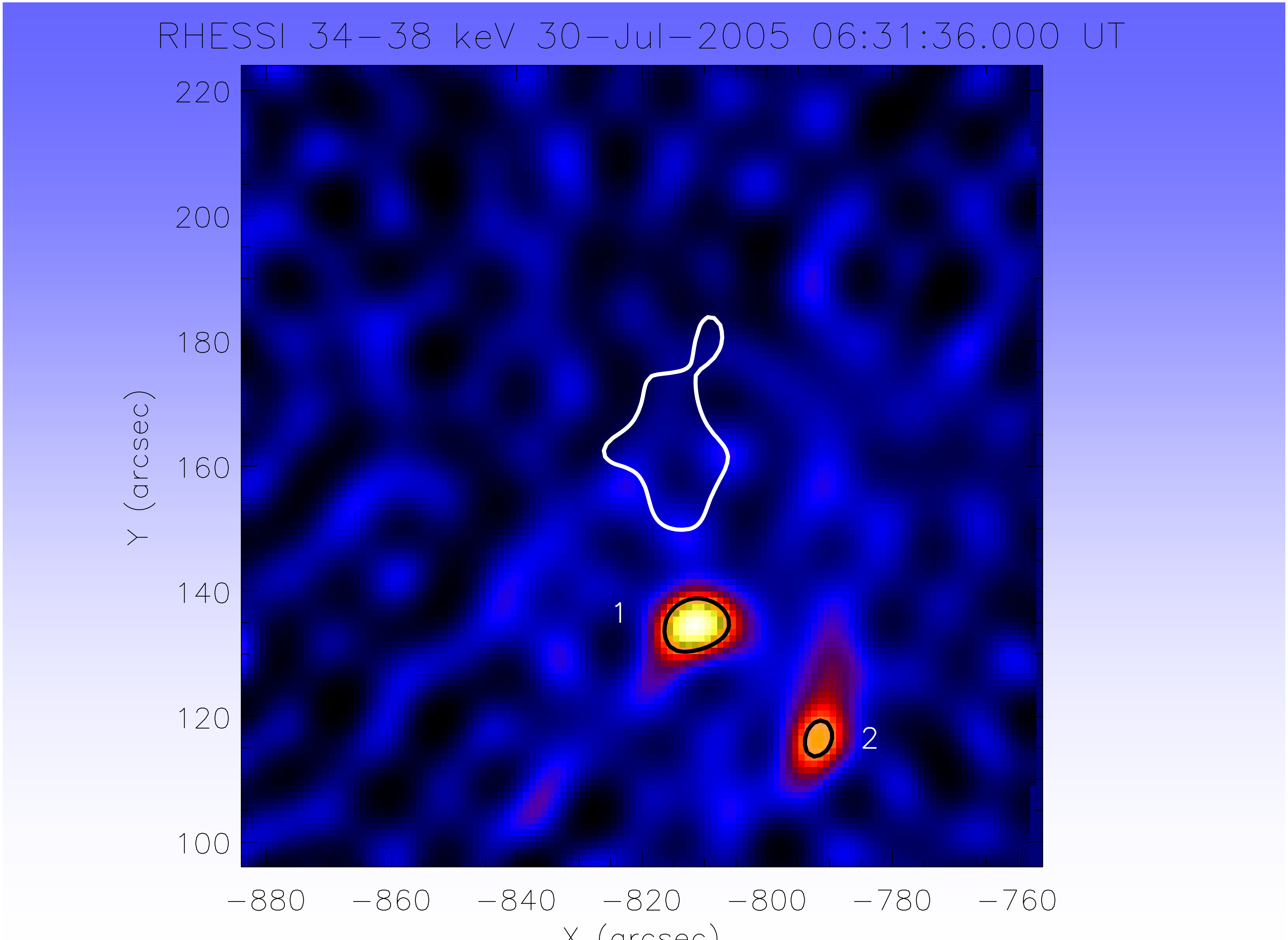
RHESSI 34–38 keV 30–Jul–2005 06:31:36.000 UT
220
200
180
160
140
120
100
Y (arcsec)
1
2
−880
−860
−840
−820
−800
−780
−760
X (arcsec)

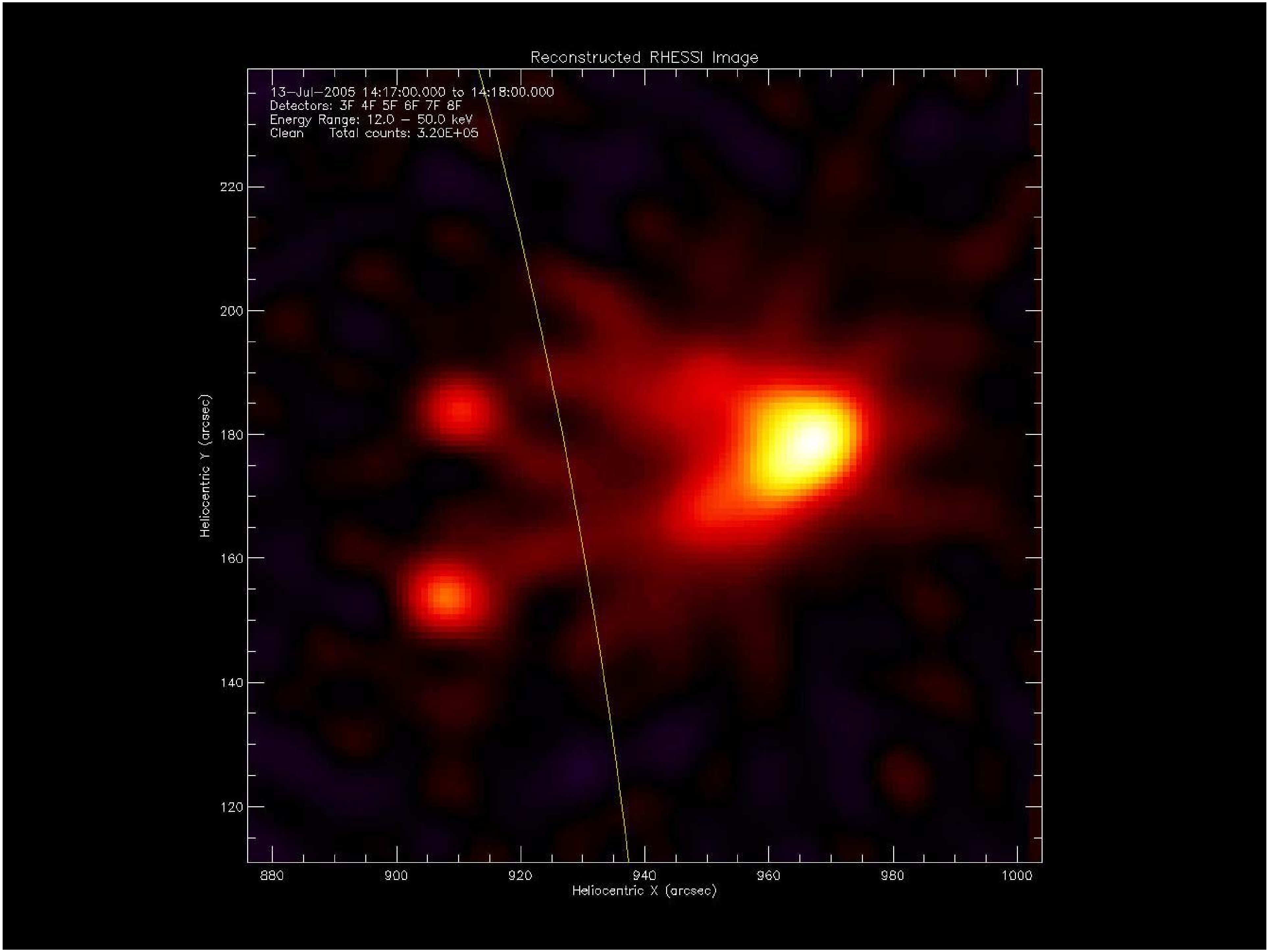
Reconstructed RHESSI Image
13-Jul-2005 14:17:00.000 to 14:18:00.000
Detectors: 3F 4F 5F 6F 7F 8F
Energy Range: 12.0 - 50.0 keV
Clean Total counts: 3.20E+05
Heliocentric Y (arcsec)
220
200
180
160
140
120
880
900
920
940
960
980
1000
Heliocentric X (arcsec)